

Performance Limits of Differential Power Processing

Ping Wang, Minjie Chen
Princeton University

Abstract: This paper studies the performance limits of differential power processing (DPP). A stochastic model is developed to evaluate the expected loss of DPP topologies with probabilistic load distribution. The performance limits of several DPP topologies are derived and compared with rigorous assumptions on semiconductor die area and magnetic volume. The impacts of the load distribution and load scale on the performance limits are investigated. The theoretical derivation is verified with numerical simulations and experimental results. The performance limits of DPP topologies are quantified, providing generalized design guidelines for differential power processing.

1 Introduction

Differential power processing (DPP) has been proved effective in many applications including solar photovoltaics, battery management systems, and IT equipments on server racks (Fig. 1) [1–4]. DPP converters only process the differential power and can greatly reduce the power conversion stress and loss. Various DPP topologies have been explored, with tradeoffs in efficiency, size, cost, and control complexity. Empirical work has been done to compare DPP converters with traditional dc-dc converters using numerical and SPICE simulations [2, 3]. An analytical model providing generalized design guidelines for DPP topologies under a set of rigorous assumptions is needed and is the main focus of this paper.

This paper systematically investigates the performance limit of differential power processing. A performance scaling factor, $\mathcal{S}(\bullet)$, is introduced to describe how the performance of a DPP converter changes as the system size scales up. The model has a minimum set of assumptions, offers rich design insights, and is verified with numerical simulations and experimental results. Extended theoretical derivations, modeling details, and experimental results will be provided in the full paper.

2 Stochastic Loss Model and Scaling Factor of DPP Topologies

Fig. 2 shows several example DPP topologies classified into two categories: 1) direct DPP, in which there is a direct power flow between two arbitrary units; and 2) indirect DPP, in which the power is processed by numerous standalone dc-dc converters. Fig. 2a–2c are direct DPP topologies, and Fig. 2d is an indirect DPP topology. DPP solutions are typically applied to modular energy systems with stochastic loads (solar cells, battery cells, servers). We develop a generalized analysis framework for DPP systems with numerous series-stacked voltage domains and stochastic loads, and compare the results against a conventional dc-dc converter functioning as a dc transformer.

The DPP system in Fig. 1 has N series-stacked voltage domains, each comprising M loads connected in parallel. The voltage of each voltage domain is V_0 . Assume that the instantaneous power of the j^{th} load in the i^{th} voltage

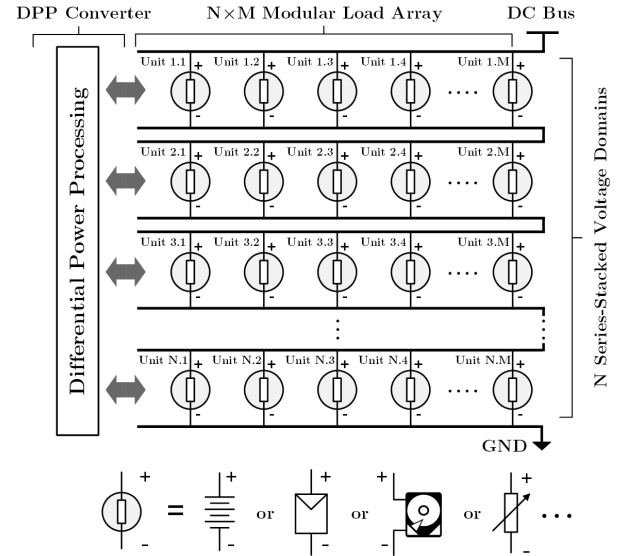


Fig. 1: A $N \times M$ differential power processing system with N series-stacked voltage domains, each comprising M modular loads. The modular load units can be battery cells, PV panels, or hard disk drives (HDD).

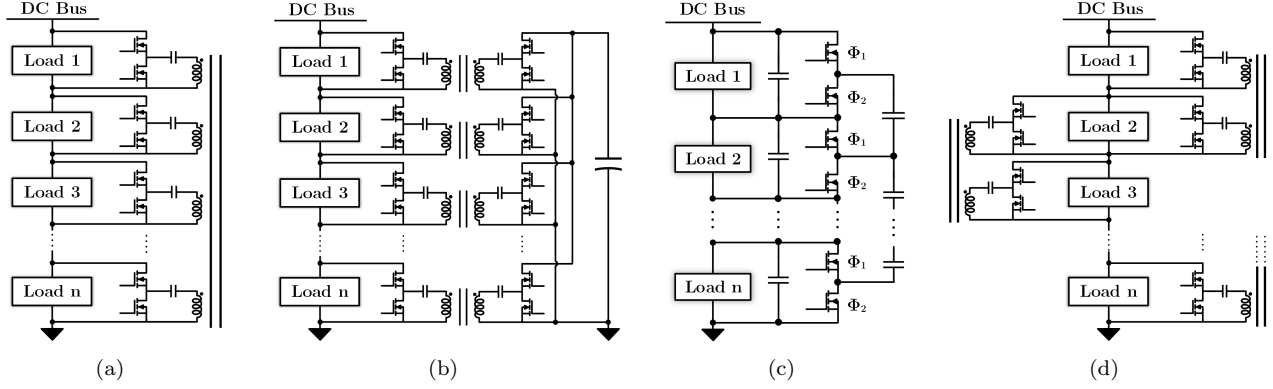


Fig. 2: Example DPP topologies: (a) ac-coupled direct DPP [4]; (b) dc-coupled direct DPP [2]; (c) switched-capacitor based [5] direct DPP; (d) dual-active-bridge [6] based ladder indirect DPP. There are many different ways of implementing these topologies [1–5].

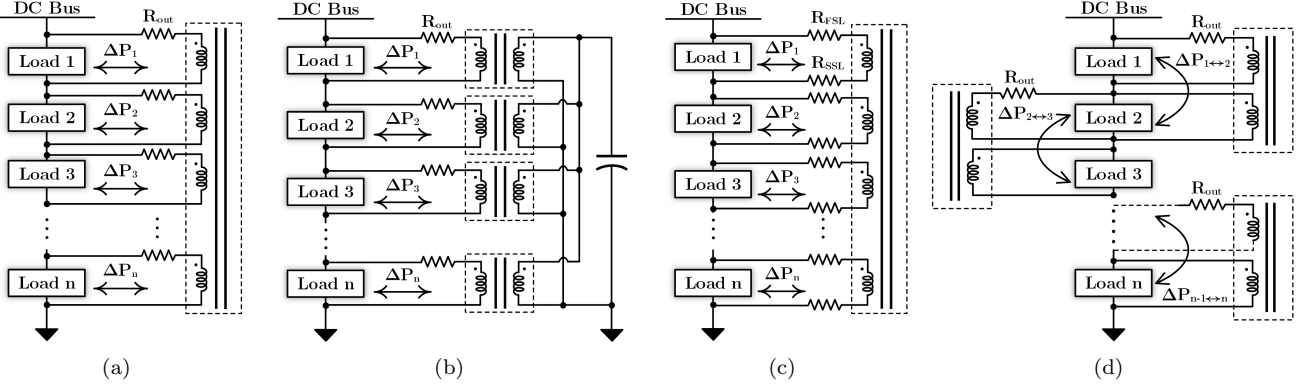


Fig. 3: Simplified models of DPP topologies with the converter modeled as an ideal transformer and an output resistance: (a) ac-coupled direct DPP; (b) dc-coupled direct DPP; (c) switched-capacitor based direct DPP; (d) dual-active-bridge based indirect DPP.

domain is $P_{ij}(t)$. $P_{ij}(t)$'s are *independent and identically distributed* (i.i.d) random variables. The total power consumed by the i^{th} voltage domain is the summation of the M random variables: $P_i(t) = P_{i1}(t) + P_{i2}(t) + \dots + P_{iM}(t)$. To balance the series-stacked voltage domains, differential power should be processed. The instantaneous differential power of the i^{th} voltage domain is the difference between its power and the average power of all voltage domains:

$$\Delta P_i(t) = \frac{P_1(t) + P_2(t) + \dots + P_N(t)}{N} - P_i(t) = \bar{P}(t) - P_i(t). \quad (1)$$

$\Delta P_i(t)$ is the power processed by the DPP converter and is directly related to the conduction loss of the DPP converter. We derive the conduction losses of several example topologies as a function of $\Delta P_i(t)$.

• **Direct-Coupled DPP Converter:** A direct-coupled DPP topology can be modeled as an N -port network with all ports connected to an N -winding ideal transformer of uniform turns ratio as shown in Fig. 3a (which is functionally equivalent to Fig. 3b and Fig. 3c). The conduction loss of the DPP converter can be captured by an output resistance R_{out} , which is assumed to be identical for all ports. In a direct-coupled DPP converter, the i^{th} port is processing a differential power of $\Delta P_i(t)$, and the total conduction loss of the full N -port DPP system is:

$$P_{loss}(t) = R_{out} \sum_{i=1}^N \Delta I_i(t)^2 = R_{out} \sum_{i=1}^N \left(\frac{\Delta P_i(t)}{V_0} \right)^2 = \frac{R_{out}}{V_0^2} \sum_{i=1}^N (P_i(t) - \bar{P}(t))^2. \quad (2)$$

$P_{loss}(t)$ reflects the variance of an independently repeated sampling experiment of the random variable $P_i(t)$. Its

expectation, the average power loss of the DPP system over a long enough period, is:

$$\mathbb{E}[P_{loss}(t)] = \frac{R_{out}}{V_0^2} \times \mathbb{E} \left[\sum_{i=1}^n (P_i(t) - \bar{P}(t))^2 \right] = M(N-1) \frac{R_{out}}{V_0^2} \sigma^2(P_{ij}(t)) \Rightarrow \underbrace{\mathcal{S}(MN)}_{\text{scaling factor}}, \quad (3)$$

where $\sigma^2(P_{ij}(t))$ is the variance of P_{ij} . We use symbol $\mathcal{S}(\bullet)$ to represent the performance scaling factor of a DPP system, which illustrates the growth rate of the loss as the dimension of the DPP system increases. Eq. (3) indicates that the performance scaling factor of a $M \times N$ direct-coupled DPP system is $\mathcal{S}(MN)$. The expected loss of a direct-coupled DPP converter is only determined by the variance of each individual load, and scales linearly with M and N . The expected loss is independent from the total power of the system.

• **Indirect-Coupled DPP Converter:** In an indirect-coupled DPP topology, each DPP unit is a dc-dc converter as shown in Fig. 2d (equivalent as Fig. 3d). Power needs to go through multiple dc-dc converters from one domain to another domain. The differential power that the i^{th} DPP unit needs to process between the i^{th} and the $(i+1)^{th}$ voltage domains is $\Delta P_{i \leftrightarrow i+1}(t) = \sum_{k=1}^i (\bar{P}(t) - P_k(t)) = i \times \bar{P}(t) - \sum_{k=1}^i P_k(t)$, and the total conduction loss is:

$$P_{loss}(t) = R_{out} \sum_{i=1}^{n-1} \Delta I_{i \leftrightarrow i+1}^2 = R_{out} \sum_{i=1}^n \left(\frac{\Delta P_{i \leftrightarrow i+1}(t)}{V_0} \right)^2 = \frac{R_{out}}{V_0^2} \sum_{i=1}^{n-1} \left(i \times \bar{P}(t) - \sum_{k=1}^i P_k(t) \right)^2. \quad (4)$$

Its expectation, the average power loss of the DPP system over a long enough period, is:

$$\mathbb{E}[P_{loss}(t)] = \frac{R_{out}}{V_0^2} \times \mathbb{E} \left[\sum_{i=1}^{n-1} \left(i \times \bar{P}(t) - \sum_{k=1}^i P_k(t) \right)^2 \right] = \frac{M(N-1)(N+1)}{6} \frac{R_{out}}{V_0^2} \sigma^2(P_{ij}(t)) \Rightarrow \underbrace{\mathcal{S}(MN^2)}_{\text{scaling factor}}. \quad (5)$$

The conduction loss of a indirect-coupled DPP increases linearly as M increases, and increases quadratically as N increases, so the performance scaling factor of an $M \times N$ indirect-coupled DPP topology is $\mathcal{S}(MN^2)$. The expected loss of an indirect-coupled DPP topology is only determined by the variance of each individual load. It scales linearly with M , and scales quadratically with N , and is independent from the total power of the system.

• **Conventional N:1 Dc-Dc Converter:** In a conventional N:1 dc-dc converter, the full power of the $M \times N$ load array needs to be processed by the dc-dc converter. Assuming the output resistance of a conventional N:1 dc-dc converter is R_{out} , the conduction loss of this converter when processing power for $M \times N$ i.i.d. loads is:

$$\mathbb{E}[P_{loss}(t)] = \frac{R_{out}}{V_0^2} \times \mathbb{E} \left[\left(\sum_{i=1}^n P_i(t) \right)^2 \right] = (MN\sigma^2(P_{ij}(t)) + M^2N^2\mu^2(P_{ij}(t))) \times \frac{R_{out}}{V_0^2} \Rightarrow \underbrace{\mathcal{S}(M^2N^2)}_{\text{scaling factor}}, \quad (6)$$

where the $\mu(P_{ij}(t))$ is the average power of each unit. The expected loss of a N:1 dc-dc converter is determined by the square of the total output power and the variance of each load, and scales quadratically with M and N .

Eq. (3), (5) and (6) reveal that the average conduction losses of DPP architectures is independent from the total load power $MN\mu(P_{ij})$, validating the fundamental difference between a DPP solution and a $N : 1$ dc-dc solution, i.e. a DPP solution only processes the differential power. If the load has no variation, a DPP system is lossless.

Table 1: Output Resistance, Expected Loss, and Scaling Factor of a few DPP Topologies and a $N : 1$ DAB Converter

	Topology	Output Resistance	Expected Loss	Scaling Factor
Direct-Coupled	Ac-Coupled	$\frac{8N}{G_{SW}} + \frac{4N}{G_M}$	$M(N-1)\sigma^2(P_{ij}(t)) \times \frac{R_{out}}{V_0^2}$	$S(MN)$
	Dc-Coupled	$\frac{32N}{G_{SW}} + \frac{16N}{G_M}$		
	SC-based	$\frac{8N}{G_{SW}}$		
Indirect-Coupled	DAB-based	$\frac{32N-32}{G_{SW}} + \frac{16N-16}{G_M}$	$\frac{M(N-1)(N+1)}{6} \sigma^2(P_{ij}(t)) \times \frac{R_{out}}{V_0^2}$	$S(MN^2)$
N:1 Converter	DAB	$\frac{32}{G_{SW}} + \frac{16}{G_M}$	$(MN\sigma^2(P_{ij}(t)) + M^2N^2\mu^2(P_{ij}(t))) \times \frac{R_{out}}{V_0^2}$	$S(M^2N^2)$

3 Performance Limits, Simulation Verification, and Experimental Results

We compare the performance limits of a variety of different differential power processing topologies basing on the following assumptions: (a) All topologies have identical semiconductor die area represented by $\sum G_{sw} V_{sw}^2$ (G_{sw} is the switch conductance; V_{sw} is the switch voltage rating) [5]; all $\sum G_{sw} V_{sw}^2$'s are normalized to $G_{SW} V_0^2$. (b) All topologies have identical total magnetic window areas represented by $\sum G_m$ (G_m is the conductance of each winding); all $\sum G_m$'s are normalized to G_M . One way to design an optimal dc-dc converter is to equally allocate the semiconductor die area and transformer window area between input and output ports, and make the design as symmetric as possible. Following the methods used in [5], we derive the output resistance of the four example DPP topologies in Fig. 2, as well as the output resistance of a dual-active-bridge (DAB) based $N : 1$ dc-dc converter. The effective output resistances are used to compare the conduction losses of different topologies. The expected losses of several DPP topologies in Fig. 2 are listed in Table 1. Detailed derivations will be provided in the full paper.

We use the ratio between the expected loss of a DPP converter and the expected loss of the $N : 1$ DAB converter (namely the Ratio-of-Loss ($ROL = \frac{P_{loss,DPP}}{P_{loss,DAB}}$)) as a figure-of-merit to evaluate the performance of DPP topologies. The coefficient of variance C_V of $P_{ij}(t)$ is $\frac{\sigma(P_{ij}(t))}{\mu(P_{ij}(t))}$. The ROLs of a few DPP topologies are shown in Fig. 4. A lower ROL indicates lower loss or smaller volume. Monte Carlo simulations are performed to validate the stochastic loss model. The simulations are executed 10,000 times to obtain the average conduction losses of different topologies. The simulated ROL matches precisely with the ROL predicted by the theoretical models.

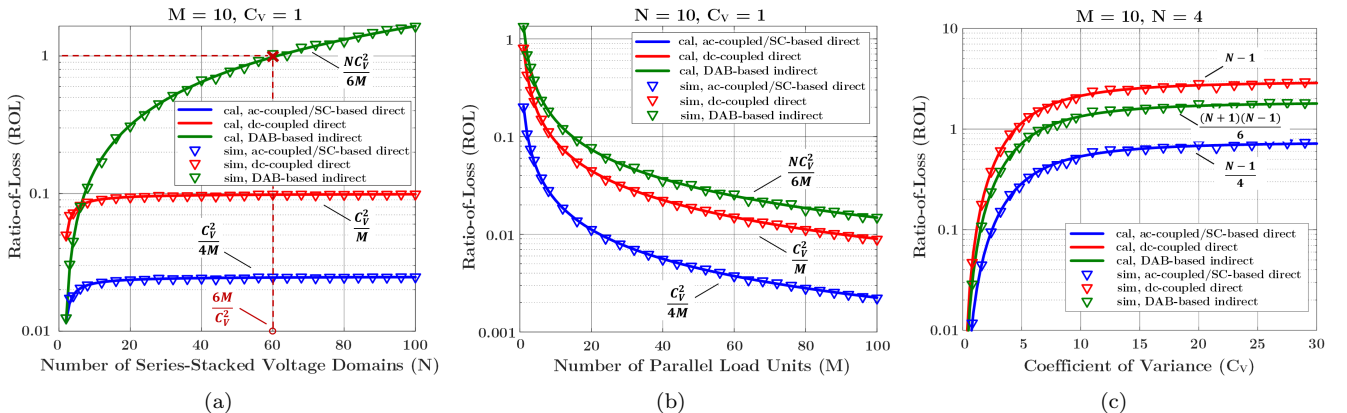


Fig. 4: Calculated (-) and simulated (∇) Ratio-of-Loss ($ROL = \frac{P_{loss,DPP}}{P_{loss,DAB}}$) as functions of: (a) the number of series-stacked voltage domains (N); (b) the number of parallel modular loads within one voltage domain (M); (c) coefficient of variance (C_V) of the loads.

Fig. 4a and 4b show the ROL of different DPP topologies as N or M increases. As N increases, the ROL of the direct-coupled DPP topologies (blue and red) converges to a constant, while the ROL of the indirect-coupled DPP topology (green) keep on increasing. The ROL of the ac-coupled & SC-based direct-coupled DPP topology converges at $\frac{C_V^2}{4M}$, and the ROL of the dc-coupled direct DPP converges at $\frac{C_V^2}{M}$. This graph provides quantitative design insights for DPP architectures. For example, with $M = 10$ and $N \geq 2$, if $C_V = 1$, the ROL of an ac-coupled or SC-based direct DPP converter is lower than $1/40$, indicating over 40x loss reduction from a $N : 1$ dc-dc converter. Similarly, a dc-coupled direct DPP converter can offer over 10x reduction in loss compared to a $N : 1$ dc-dc converter. Fig. 4c shows the ROLs of a few different DPP topologies if C_V changes. As C_V increases, the DPP converter

needs to process more differential power. The ROLs of all DPP topologies increase, but will approach an upper limit. This is because the conduction loss of a $N : 1$ converter when C_V is large is dominated by $MN\sigma^2$, increasing at the same rate as that of DPP converters. Fig. 4 reveals that the ac-coupled DPP stands out from all DPP implementations. Switched-capacitor based DPP is equally good if capacitor charge sharing loss is neglected. Fig. 5 shows the picture of a 10-port Multiport-Ac-Coupled DPP (MAC-DPP) converter powering a 10×5 hard-disk-drive storage server. A hardware-in-the-loop (HIL) test platform has been developed to enable stochastic loss analysis. The 450 W MAC-DPP system reaches a peak efficiency of 99.5% with over 630 W/in^3 power density.

4 Conclusions

This paper investigates the performance limits of differential power processing (DPP). A stochastic model is developed to evaluate the performance limits of DPP topologies as the variance (C_V) and dimension (M, N) of modular load array scales up. The performance limits of many DPP topologies are derived and compared, providing useful design guidelines for implementing DPP systems. The theoretical model is verified by Monte Carlo simulations. Extended theoretical derivations and experimental results will be presented in the final paper.

References

- [1] P. S. Shenoy and P. T. Krein, "Differential Power Processing for DC Systems," *IEEE Transactions on Power Electronics*, vol. 28, no. 4, pp. 1795-1806, April 2013.
- [2] E. Candan, P. S. Shenoy and R. C. N. Pilawa-Podgurski, "A Series-Stacked Power Delivery Architecture with Isolated Differential Power Conversion for Data Centers," *IEEE Transactions on Power Electronics*, vol. 31, no. 5, pp. 3690-3703, May 2016.
- [3] K. A. Kim, P. S. Shenoy and P. T. Krein, "Converter Rating Analysis for Photovoltaic Differential Power Processing Systems," *IEEE Transactions on Power Electronics*, vol. 30, no. 4, pp. 1987-1997, April 2015.
- [4] P. Wang, Y. Chen, P. Kushima, Y. Elasser, M. Liu and M. Chen, "A 99.7% Efficient 300 W Hard Disk Drive Storage Server with Multiport Ac-Coupled Differential Power Processing (MAC-DPP) Architecture," *2019 IEEE Energy Conversion Congress and Exposition (ECCE)*, Baltimore, MD, USA, 2019, pp. 5124-5131.
- [5] M. D. Seeman and S. R. Sanders, "Analysis and Optimization of Switched-Capacitor DC-DC Converters," *IEEE Transactions on Power Electronics*, vol. 23, no. 2, pp. 841-851, March 2008.
- [6] R. W. A. A. De Doncker, D. M. Divan and M. H. Kheraluwala, "A Three-Phase Soft-Switched High-Power-Density DC/DC converter for High-Power Applications," *IEEE Transactions on Industry Applications*, vol. 27, no. 1, pp. 63-73, Jan.-Feb. 1991.

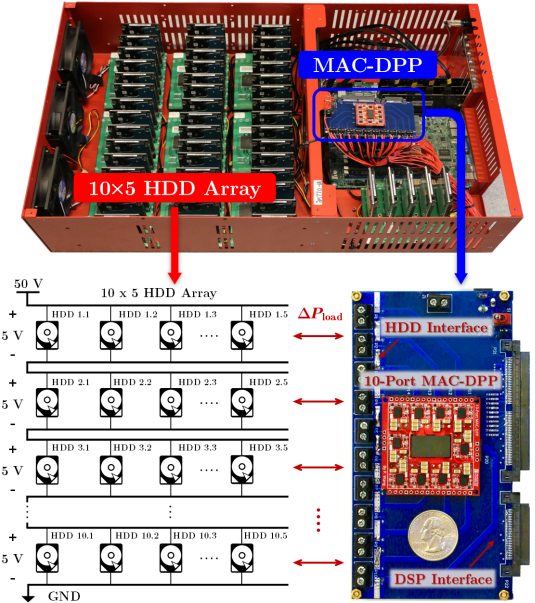


Fig. 5: A 50-HDD storage server supported by a 10-port MAC-DPP prototype with 450 W power rating and over 99.5% peak system efficiency.